Surface Chemistry in the Atomic Layer Deposition of TiN Films from $TiCl_4$ and Ammonia

Hugo Tiznado and Francisco Zaera*

Department of Chemistry, University of California, Riverside, California 92521

Received: March 31, 2006; In Final Form: May 17, 2006

The surface chemistry of atomic layer depositions (ALD) of titanium nitride films using alternate doses of $TiCl_4$ and NH_3 was characterized by using X-ray photoelectron spectroscopy. The nature of the species deposited by each half-reaction was explored first. Evidence was obtained for the partial loss of chlorine atoms and the reduction of the metal during the adsorption of the $TiCl_4$. Subsequent ammonia treatment removes most of the remaining chlorine and leads to the formation of a nitride. Both half-reactions were proven self-limited, stopping after the deposition of submonolayer quantities of the materials. Repeated ALD cycles were shown to lead to the buildup of thick films. However, those films display a Ti_3N_4 layer on top of the expected TiN. The data suggest that the reduction of the Ti^{4+} species may therefore occur during the $TiCl_4$, not NH_3, dosing step. The incorporation of impurities in the films was also investigated. Chlorine is only deposited on the surface, and in negligible quantities. This Cl appears to originate from readsorption of the HCl byproduct, and could be removed by light sputtering, heating, or further ammonia treatment. Oxygen incorporation, on the other hand, was unavoidable and was determined to possibly come from diffusion from the underlying substrate.

1. Introduction

The continuing scaling down of microelectronic chips and other semiconductor devices keeps imposing increasingly more stringent requirements on the methods used for the deposition of thin films. As microelectronic manufacturing enters the nanoscale node, a need arises for deposition techniques to produce good thin and conformal films at low growth temperatures. Physical vapor deposition (PVD) methods are still widely used for these applications but usually display a directionality incompatible with the conformal coating of rough topographies.[1] Chemical vapor deposition (CVD) processes offer an interesting alternative but typically require too high temperatures, lead to the deposition of high levels of contaminants, and are often difficult to control.[2] It is in this context that atomic layer deposition (ALD) has gained increasing interest in recent years.

ALD is a chemical deposition method in which two complementary self-limiting reactions are used sequentially and in alternating fashion to slowly build up solid films one monolayer at a time.[3−6] ALD was in fact initially developed in the late 1970s under the name of atomic layer epitaxy for the manufacturing of thin-film electroluminescent flat-panel displays[7] and the preparation of III−V compounds,[8] but it was only in the mid 1990s that ALD regained interest in the silicon-based microelectronics industry for the manufacturing of high aspect-ratio integrated circuits.[5,9]

There are several advantages to the use of ALD over other film deposition methods. Among them: (1) the film thicknesses depend only on the number of cycles employed, not on the exposures used in each cycle, so the control of film thickness is simplified and more accurate; (2) there is a lesser need for flux homogeneity of the reactant in the deposition reactor, so the processes are more reproducible and easy to scale for large-area coatings without sacrificing conformality; (3) there is more flexibility in the design of the operational conditions for the deposition, in particular in terms of temperature and reactant flows; (4) interferences from gas-phase reactions are often avoided because of the separation of the two half-reactions in time, and (5) ALD is easier to use for the manufacturing of layered structures. On the negative side, ALD suffers from some intrinsic limitations, including (1) the deposition of undesirable contaminants within the growing films because of the decomposition of the precursors via side reactions, (2) the growth of films with different microstructures and morphologies from those obtained by PVD, and (3) the slow nature of the deposition, at only a fraction of a monolayer per cycle.

ALD processes are quite flexible and, therefore, can potentially be tuned for the growth of virtually any kind of film. However, for an ALD process to work properly, several conditions must be fulfilled:[10] (1) The precursors need to have appropriate chemical and physical properties, namely, they must be thermally stable and sufficiently volatile for easy transport and handling and have low toxicity, explosiveness, and flammability, (2) The two reactants involved must exhibit the appropriate chemistry, namely, their surface conversion must be simple, fast, complete, irreversible, and self-limiting and must occur at suitable low temperatures, and (3) the reactions need to be complementary, that is, each needs to be able to prepare the surface for the other and to lead to the formation of films with the right stoichiometry.

Tuning ALD processes therefore requires an intimate knowledge of the surface chemistry involved. Unfortunately, most work on ALD has been empirical in nature and has focused on the characterization of the grown films rather than on the details of the deposition mechanism.[3,5] Even in the case of the growth of TiN films from $TiCl_4$ and NH_3 (Figure 1), one of the best ALDs studied to date,[11−20] many questions remain. For instance, it is not yet clear what the stoichiometry of the whole process is, how the reduction of the titanium atoms (from Ti^{4+} in $TiCl_4$ to Ti^{3+} in TiN) occurs, or what the oxidation byproduct is. It

* Corresponding author. Phone: (951) 827-5498. Fax: (951) 827-3962. E-mail: zaera@ucr.edu.

10.1021/jp062019f CCC: $33.50 © 2006 American Chemical Society
Published on Web 06/17/2006

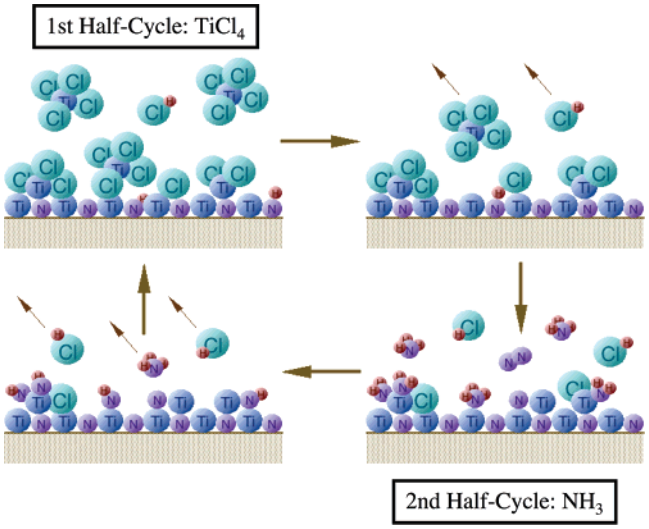

Figure 1. Schematic representation of the atomic layer deposition process discussed in this report for the growth of titanium nitride films using $TiCl_4$ and NH_3.

has also not been clearly established what the sources of the contaminants are or how they get incorporated into the film. Not even the specific composition and stoichiometry of the deposited film has been properly determined. Here, we report on results from surface-science research aimed at answering some of these questions. It was found that, although the bulk of thick titanium nitride films deposited by these $TiCl_4 + NH_3$ ALD processes have the expected TiN stoichiometry, they are covered with an outer layer of Ti_3N_4. Evidence was obtained for the reduction of the titanium atoms during the exposures to $TiCl_4$, not to ammonia (as typically believed). This suggests the possible formation of either chlorine gas or chloroamine rather than molecular nitrogen as the oxidation products. In terms of the incorporation of contaminants in the grown films, it was determined that chlorine is deposited in small quantities on the surface, most likely from readsorption of the HCl byproduct,[5] and can be easily removed by either further treatment with ammonia or heating in vacuum. Oxygen, on the other hand, was detected all throughout the grown films. Because of the careful handling of the samples in the experiments reported here, in which they were never exposed to the outside environment, it is unlikely for the oxygen to originate from post-oxidation of the film, as reported before.[15,20,21] Instead, a possible migration of oxygen from the underlying substrate into the film as it grows is suggested.

2. Experimental Section

The experiments reported here were carried out in a two-chamber stainless steel ultrahigh vacuum (UHV) apparatus briefly described elsewhere.[22] The main chamber can be evacuated to a base pressure in the 10^{-10} Torr range by using a turbomolecular pump, although it usually stood at approximately 1×10^{-9} Torr during operation. This chamber is equipped with instrumentation for X-ray photoelectron spectroscopy (XPS) and mass spectrometry for analysis of the gases. An ion gun is also available for sample cleaning and depth profiling. The samples are mounted on a supporting rod used to transfer the sample between the two chambers by traveling through a set of concentric differentially pumped seals. With this setup, transferring between the two chambers can be carried out without exposures of the samples to the outside atmosphere, and also without contaminating either chamber with the gases from the other. The transferring rod can be rotated for better alignment during XPS acquisition, and is capable of cooling to ~200 K and resistive heating to up to approximately 1000 K. The temperature of the substrate is monitored with a K-type thermocouple inserted into a small hole drilled in the copper hot plate where the substrates are placed, and held in place with a tungsten-made spring.

The XPS data are collected in the main chamber by using a Leybold EA11 multichannel detection system and a Mg Kα ($h\nu = 1253.6$ eV)/Al Kα ($h\nu = 1486.6$ eV) dual-anode X-ray excitation source. The data for the experiments with the glass and tungsten substrates were taken using the magnesium source, those on nickel and copper by employing the aluminum anode. Survey spectra (scans of 1000 eV or more in width) were taken by using a constant band-pass energy of 100.8 eV, which corresponds to a spectral resolution of 2.0 eV. Additional high-resolution scans of the Ti 2p, N 1s, Cl 2p, and O 1s regions were obtained with a band-pass energy of 31.5 eV (or, occasionally, a band-pass energy of 20.0 eV) to accurately determine their energy and shape. Taken into consideration the natural line width of the excitation source, this corresponds to a resolution of about 0.9 eV (0.8 eV for the 20.0 eV band-pass energy, as corroborated experimentally by the Ti 2p XPS peaks from TiO_2 reported in Figure 9). All of the XPS peak positions are reported in binding energies (BEs), and were calibrated relative to the reported positions of the substrate peaks and corroborated by the position of the O 1s XPS feature in oxidized samples;[23] they are deemed accurate within ±0.1 eV. The reported spectra were obtained by averaging either 10 or 100 scans for the survey or high-resolution runs, respectively. XPS peak areas were converted into relative surface atomic concentrations by using reported relative sensitivity factors.

All gases in these experiments, namely, ammonia (Matheson, anhydrous, 99.99% purity), O_2 (Airgas, ultrahigh purity), and argon (Airgas, 99.998% purity), were used as supplied, and introduced into the vacuum chamber via leak valves. The liquid $TiCl_4$ (Acros, 99.9%) was purified in situ in our gas-handling manifold by a series of freeze−pump−thaw cycles and dosed by introducing its vapor into the chamber through the same leak valve used for ammonia dosing. Four solid substrates were tested in these studies: a glass (Pyrex) microscope slide, a tungsten foil (ESPI, 0.25-mm-thick, >99.98% purity), a nickel foil (Sigma-Aldrich, 0.25-mm-thick, 99.995% purity), and an oxygen-free copper solid (taken from a copper gasket, Duniway Stockroom). They were all cut into square pieces of approximately 1 cm^2 area and placed in the sample holder within the transferring rod of our UHV system. The surfaces were cleaned by extensive argon sputtering and checked by XPS before use. Most contaminants, including adventitious carbon, could be removed by this treatment, but small amounts of oxygen were often unavoidable.

Gas dosing for the film deposition was carried out in the auxiliary chamber, which was designed to operate as the ALD reactor. This ~5 L chamber could be turbopumped to base pressures as low as 5×10^{-9} Torr, but more typically operated in the low 10^{-8} Torr range. To optimize the ALD operation and investigate the source of the contaminants in the deposited TiN films, several reactor designs were tested. First, although the reactor could be isolated from its turbopump by using a gate valve installed between the two, it was determined that continuous pumping was required to minimize contamination from gases desorbing from its walls. Experiments were also carried out with and without a continuous flow of an inert gas (argon) through the reactor. Although slightly better results were

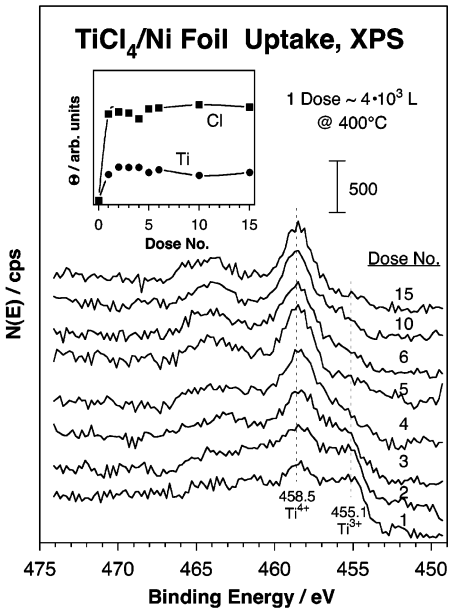

Figure 2. Ti 2p XPS for the uptake of $TiCl_4$ on a nickel foil at 400 °C. The reactant was dosed in pulses of approximately 4×10^3 L. The inset displays the relative surface concentrations of Ti and Cl as a function of the dose estimated from the XPS data. Three key observations are derived from these data: (1) The reaction is self-limiting, saturating by the second pulse; (2) the initial titanium is deposited in the form of Ti^{3+} but is converted to a +4 oxidation at saturation, and (3) the final average stoichiometry of the adsorbate species is $TiCl_{3.5}$.

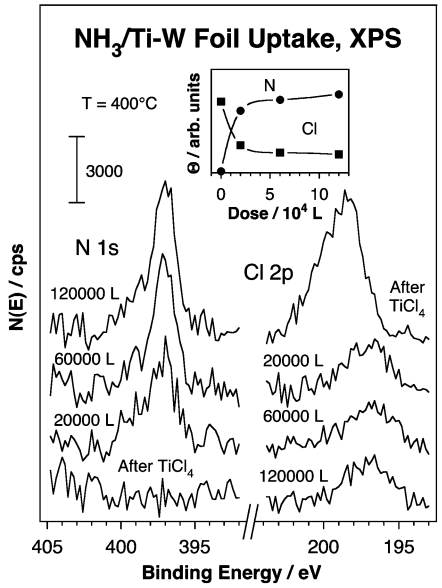

Figure 3. N 1s (left) and Cl 2p (right) XPS data for the uptake of ammonia on a tungsten film previously saturated with $TiCl_4$. Both the pretreatment and the ammonia dosing were carried out at 400 °C. The inset displays the relative surface coverages calculated from these data. The ammonia treatment removes most of the surface chlorine and deposits nitrogen in the form of a nitrate (BE = 397.1 eV).

obtained by maintaining a steady-state Ar pressure between 1×10^{-6} and 1×10^{-5} Torr at all times, the differences with the data when vacuum was maintained in the reactor between doses were not significant. The $TiCl_4$ was initially dosed by setting the pressure at a given value for a defined period of time, but this arrangement was later modified so a fixed amount of the gas was first trapped behind the leak valve and then introduced as a short pulse while still pumping on the system (typical pressure-versus-time profiles of those pulses are shown in Figure 8). Also, although dosing in the first experiments was carried out by backfilling of the reactor chamber, this was later improved by using a dosing tube placed above and close to the solid sample to increase the flow of the gas onto that surface and decrease the extent of its interactions with the walls of the chamber. It should be noted that in our setup only the substrate is heated and the walls of the reactor remain at room temperature. It would be expected that this would minimize the desorption of contaminants from the walls, but there is still the risk of displacing those adsorbates during dosing, as discussed below. An attempt was made to minimize the reactor volume further by attaching a cap to the doser capable of sealing a small ($\sim$1 cm^3) volume around the sample, but this resulted in a worsening of the contamination problems, presumably because of the increased surface-to-volume ratio of this arrangement. Finally, it should be mentioned that, because $TiCl_4$ is quite corrosive, a cold trap needed to be placed between the reactor and the turbopump to condense the unused gases.

3. Results

3.1. Chemistry of Each ALD Half-Cycle Reaction. The chemistry of each individual reaction in the $TiCl_4 + NH_3$ ALD process (Figure 1) was characterized first. Figure 2 displays the Ti 2p XPS data obtained during the uptake of $TiCl_4$ on a nickel foil at 400 °C. Traces are displayed for each individual $TiCl_4$ dose, which consisted of pulses of approximately $(4 \pm 1) \times 10^3$ L ($P_{max} \sim 1 \times 10^{-4}$ Torr, $\Delta t \sim 40$ s; 1 L = 1×10^{-6} Torr s). The uptake of both titanium and chlorine was estimated by integration of the respective Ti 2p and Cl 1s XPS signals (chlorine data not shown) and plotted versus the number of pulses in the inset. Those results highlight the self-limiting nature of the adsorption: surface saturation levels are reached for both elements after only a couple of pulses. Also to note from these data is the fact that, although most traces are dominated by a peak at 458.5 eV typical of the Ti $2p_{3/2}$ XPS photoelectrons from titanium in a +4 oxidation state (as is the case in $TiCl_4$),[23] the first few display a prominent feature at 455.1 eV more characteristic of Ti^{3+}. This indicates an initial reduction of the $TiCl_4$, at least on metal surfaces, and strongly suggests dissociative adsorption and the formation of $TiCl_3$(ads) species. This conclusion is supported by the atomic composition of the monolayer determined from the saturation concentrations of Ti and Cl on the surface, which amounted to a ratio of approximately Cl/Ti $\sim$ 3.5. Evidence for $TiCl_4$ dissociative adsorption has been previously reported on W(100)[24] and W(110),[25] and also on Si(100).[26]

Figure 3 reports the N 1s (left) and Cl 2p (right) XPS traces recorded during the uptake of ammonia on a tungsten foil previously saturated with $TiCl_4$. Both $TiCl_4$ and NH_3 exposures were carried out at 400 °C. Again, the relative coverages of those atoms on the surface were estimated from the areas of the XPS peaks and plotted as a function of dose in the inset. A nitrogen peak grows around 397.1 eV, a value typical of metal nitrides,[23] and saturates after exposures of about 5×10^4 L. Most of the chlorine, which initially shows as a peak at 198.3 eV, is removed by this ammonia treatment, but a small (a few percent of a monolayer) and broad feature remains in the XPS spectra at about 196.8 eV even after NH_3 exposures over 10^5 L.

The sequence of steps that constitute one cycle in the ALD process is exemplified by the data in Figure 4. An XPS trace was obtained after each step, including the pumping stages between the two half-reactions (for the reaction steps, the sample

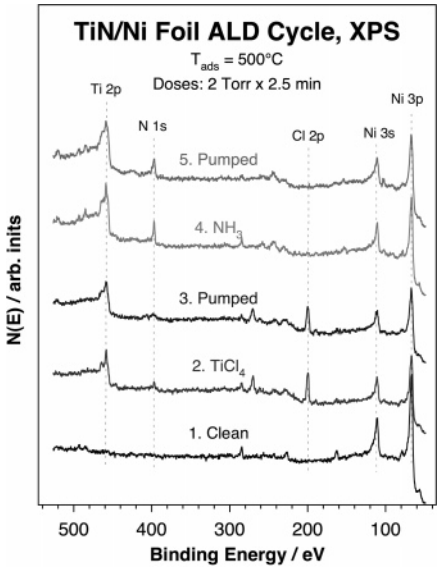

Figure 4. XPS data after each step of the ALD cycle. The expected behavior is corroborated, including the deposition and persistence of Ti and Cl after $TiCl_4$ dosing and pumping and the replacement of the chlorine by nitrogen upon ammonia treatment.

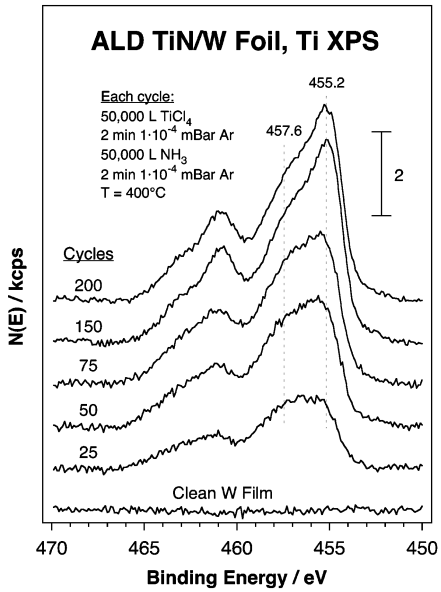

Figure 5. Ti 2p XPS versus the number of ALD cycles on a tungsten foil. The details of the steps in each cycle are provided in the figure. The signals for Ti^{3+} (Ti $2p_{3/2}$ BE = 455.2 eV) and Ti^{4+} (BE = 457.6 eV) are seen in approximately equal proportions after 25 cycles, but only the signal for the latter grows after that.

was transferred to the analysis chamber while the gas was still present in the reactor volume). The expected behavior is corroborated by these data. First, exposure of the clean nickel foil to $TiCl_4$ leads to the growth of XPS peaks for both titanium (Ti 2p, BE ~ 458 eV) and chlorine (Cl 2p, BE ~ 198 eV). The Ti 2p XPS feature also displays the complexity that arises from a mixture of Ti^{3+} and Ti^{4+} surface species, as discussed above. All of these peaks survive further pumping in vacuum, but the spectra change upon ammonia treatment, at which point the chlorine peaks are replaced by a new feature for N 1s photoelectrons (BE ~ 397 eV). Note that the Ni XPS peaks in this spectrum become more intense at this point than those right after the $TiCl_4$ exposure, presumably because of the attenuation of the Ti 2p photoelectrons by the surface chlorine atoms. The top trace in Figure 4 was acquired after the end of the ALD cycle, and indicates the deposition of a submonolayer quantity of titanium nitride. Although in this particular example a temperature of 500 °C was used, similar qualitative results were seen at lower temperatures.

3.2. Titanium Nitride Film Deposition. Thick titanium nitride films were grown in several substrates by repeating the ALD cycles described above many times. Typical Ti 2p XPS data from one of such processes are shown in Figure 5 at different stages of the deposition. After 25 cycles, a broad peak between 454 and 460 eV is seen for the Ti $2p_{3/2}$ photoelectrons. This peak could be deconvoluted into two features of approximately equal intensity centered at 455.2 and 457.6 eV, corresponding to Ti^{3+} and Ti^{4+} surface species, respectively. The film thickness at this point, calculated by both the intensities of the Ti 2p and N 1s XPS peaks and the attenuation of the W 4f XPS signal, is estimated at ~0.8 nm. Additional ALD cycles resulted in a total increase in Ti 2p and N 1s XPS signal intensities, mostly in the Ti^{3+} peak in the case of the Ti $2p_{3/2}$ feature. The Ti^{3+} peak at 455.2 eV is certainly the dominant feature in all of the spectra after 50 or more ALD cycles, but the Ti^{4+} signal at 457.6 eV never disappears and still accounts for approximately 40% of the total Ti $2p_{3/2}$ XPS intensity after 200 cycles, at which point the film is close to 8 nm in thickness.

Depth profiles of the final films were performed by recording XPS spectra as a function of time of sputtering using 5 keV Ar^+ ions. Typical data for this are shown in Figure 6, in this

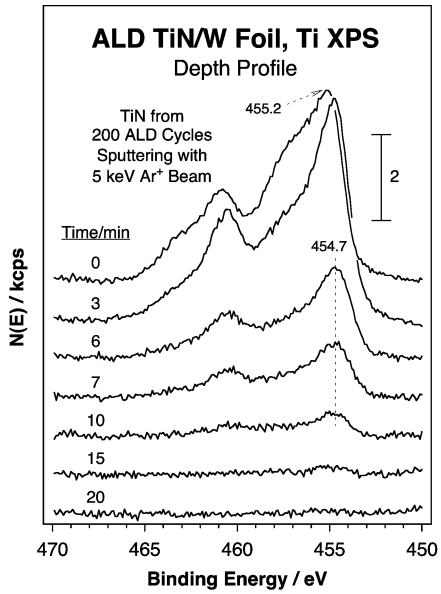

Figure 6. Ti 2p XPS as a function of sputtering time in depth-profile studies of an ~8-nm-thick titanium nitride film grown by the ALD process. Selective removal of the Ti^{4+} species is seen within the first 3 min, and total film removal is accomplished after 20 min.

case for a film like that produced by the process described in the previous paragraph. A striking change is seen after only 3 min of sputtering, with the Ti $2p_{3/2}$ XPS spectra losing most of the Ti^{4+} contribution at 457.6 eV. The peak due to Ti^{3+} also sharpens up and shifts down to 454.7 eV. Continuing sputtering leads to a decrease in the total Ti (and N) XPS signal, until the spectrum for the clean tungsten substrate is restored after approximately 20 min of sputtering.

The results from quantitation of the information obtained by the experiments reported in Figures 5 (left) and 6 (right) are summarized in Figure 7. Each panel reports the average atomic compositions of the surface, the N/Ti atomic ratios, and the estimated thickness of the titanium nitride films at each step. During the deposition (left panel), an exponential decay of the concentration of tungsten from the substrate is accompanied by

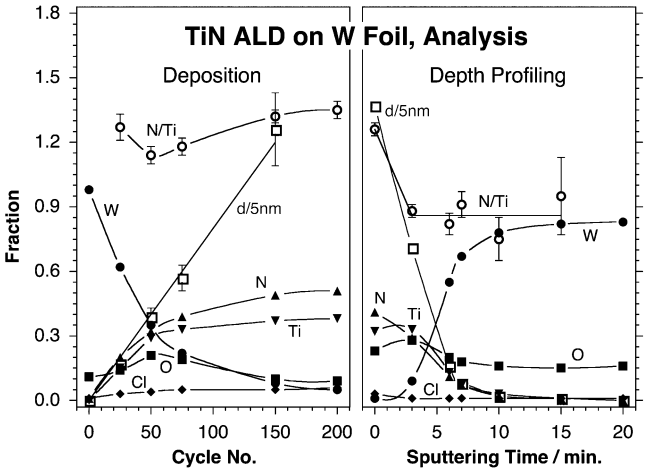

Figure 7. Summary of the data obtained from the experiments reported in Figures 5 and 6. Shown here are the average atomic compositions of the surfaces, the N/Ti atomic ratios, and the estimated film thicknesses at the different stages of deposition (left) and depth profiling (right). A deposition rate of approximately 0.04 nm/cycle was calculated from these results. N/Ti ratios higher than unity were always observed during growth, but not after light sputtering. Chlorine was seen only in small amounts on the surface and was easily removed in the initial stages of the sputtering. Larger amounts of oxygen were detected all throughout the film.

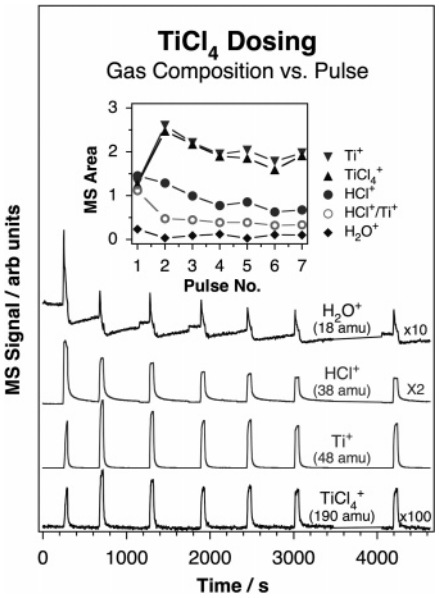

Figure 8. Mass spectrometry analysis of $TiCl_4$ during its introduction into the reactor. The signals for 18 (water), 38 (HCl), 48 (Ti), and 190 ($TiCl_4$) amu were followed as the reactant was dosed in pulses approximately 40 s in duration and 10 min apart. The measured intensities versus pulse number are summarized in the inset. $TiCl_4$ dosing displaces some water from the walls of the chamber and produces some HCl, but does not lead to significant amounts of titanium-containing gas species other than the original $TiCl_4$.

exponential growths of the signals for titanium and nitrogen. This indicates a constant rate of deposition, estimated at approximately 0.04 nm/cycle by the calculation of signal attenuation using appropriate photoelectron mean free paths.[27] It should be mentioned here that the deposition rate in these ALD processes was difficult to reproduce, because $TiCl_4$ has the tendency to adsorb on the walls of the reactor and re-desorb during the ammonia treatment, causing additional TiN growth via a regular CVD process. Faster growth rates were indeed seen with higher background pressures in the reactor, and also if the cycles were carried out without proper pumping or purging between the half-cycles. Nevertheless, the deposition rates reported in Figure 7 are consistent with ALD processes and agree quite well with those reported previously.[28]

The stoichiometry of the film varied slightly during the ALD growth but was always richer in nitrogen than the N/Ti = 1.0 ratio expected for TiN (N/Ti $\sim$ 1.2−1.4). This, combined with the observation of XPS signals for Ti^{3+} and Ti^{4+} in Figure 5, points to the presence of a mixture of TiN and Ti_3N_4 on the surface. Information on the distribution of these two solids within the film was extracted from the depth profiling data. Indeed, the N/Ti ratio decreases significantly upon sputtering of the surface, and reaches a constant value of N/Ti $\sim$ 0.9 $\pm$ 0.1 before 3 min. Given that this is accompanied by the selective removal of the Ti^{4+} species (Figure 6), it is concluded that the Ti_3N_4 sits on top of the TiN film. Recall that it is the Ti^{4+} species that appears first during the deposition process as well (Figure 5). The Ti_3N_4 top layer is estimated to be about 0.2−0.3-nm-thick at all times during the film growth.

The sputtering rate determined from film thickness calculations is approximately 1.0 nm/min. This rate is initially constant, but removal of the last vestiges of Ti and N from the deposited film takes a much longer time than expected. Another point to be mentioned from these experiments is the fact that only traces of chlorine were detected at all times and that these could be removed by heating of the sample in vacuum, by additional treatments in ammonia or by light sputtering (Figure 7, right). It appears that the surface chlorine originates from readsorption of the HCl byproduct of the ALD reactions. On the other hand, significant amounts of oxygen, up to 20 atom % in some instances, were always detected and, according to the depth profiling data, were present all throughout the film. This point will be addressed below.

3.3. Source of Contaminants. One aspect of this $TiCl_4$ + NH_3 ALD process repeatedly mentioned in past studies is the incorporation of impurities in the grown films. We looked into this issue in some detail here. For one, a number of experimental setups were tried to minimize the problem, as already mentioned in the Experimental Section. The purity of the gases was also carefully monitored. It was found that, although the $TiCl_4$ used in these experiments was quite pure, it displayed some chemistry upon introduction into the vacuum chamber. This is indicated by the mass spectroscopic analysis reported in Figure 8. There, selected masses were followed as the reactant was introduced in successive pulses, roughly 10 min apart. One thing that becomes immediately evident from those data is the increase in water partial pressure in the chamber during the pulses, most likely from displacement from the walls of the reactor by the incoming $TiCl_4$. The amount of water in the gas phase was relatively low, only a few percent of the total pressure, but enough to induce some chemistry both in the gas phase and on the surface. Indeed, some HCl was also detected in these experiments, most likely from the reaction of $TiCl_4$ with H_2O. It could be thought that the partial decomposition of the $TiCl_4$ in the gas phase may be the reason for the initial deposition of Ti^{3+} on the surface, as indicated by the data in Figure 2. However, there is no evidence that this decomposition is significant: the ratio of 48 (Ti^+) to 190 ($TiCl_4^+$) amu signals in the data in Figure 8 remains approximately constant at all times (and the same as in the mass spectra of that compound), suggesting that $TiCl_4$ is by far the major titanium-containing species in the gas phase. Perhaps more important is the potential effect that this water may have on the surface, as discussed below. It should be mentioned that all of these contamination problems could be minimized by conditioning the chamber with

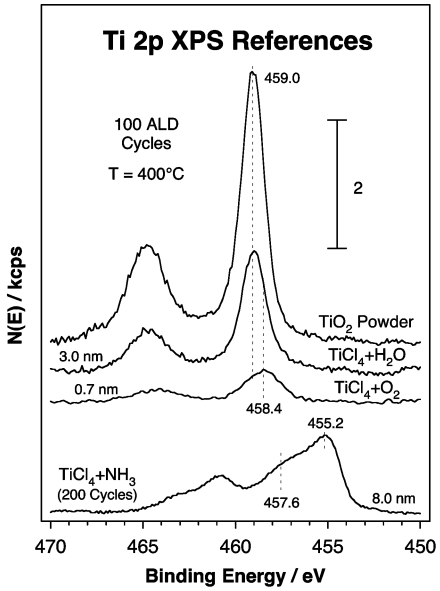

Figure 9. Ti 2p XPS data for TiO_2 films grown by $TiCl_4 + H_2O$ and $TiCl_4$ ALD processes. The spectra for a TiO_2 powder and for one of our thick TiN films are also provided for reference. The process with water is almost as efficient as that with $TiCl_4 + NH_3$, but the deposition with molecular oxygen is much slower. The Ti 2p XPS peaks for TiO_2 are at distinctively higher BEs than those seen in our TiN films, indicating that TiO_2 is not a major contaminant in those.

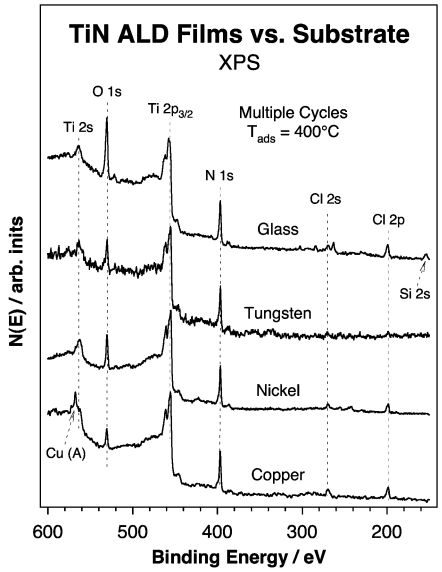

Figure 10. XPS traces covering the Ti 2s, O 1s, Ti 2p, N 1s, Cl 2s, and Cl 2p regions of the spectra for TiN films grown on four different substrates, namely (from top to bottom), glass, tungsten, nickel, and copper. Similar results were obtained in all cases, except for the levels of oxygen, which were higher on the glass sample.

$TiCl_4$ prior to the ALD experiments. Otherwise, HCl/Ti ratios as high as 100 could be observed initially (the steady-state value was measured to be about 1/3).

Despite our efforts to remove all of the contaminants from our experiments, small amounts of water were always seen in the gas phase, and oxygen incorporation in the titanium nitride films could never be avoided. Because it is well-known that TiO_2 films can be grown by using $TiCl_4 + H_2O$ mixtures,[29−32] the extent of the interference of this side reaction with the TiN ALD growth was evaluated further. Experiments similar to those with $TiCl_4 + NH_3$ were carried out with $TiCl_4 + H_2O$ and with $TiCl_4 + O_2$; the Ti 2p XPS data from the resulting films are reported in Figure 9. The growth of TiO_2 films is evident in the case of the use of water from the position of the Ti $2p_{3/2}$ XPS peak at 459.0 eV, which matches that seen for a TiO_2 powder sample (the spectrum of which is reported in the upper trace for reference). Interestingly, although this ALD process is reasonably efficient, at a rate of 0.03 nm/cycle, it is slightly slower than that for the titanium nitride deposition. The deposition with molecular oxygen is significantly less efficient, so a film only 0.7-nm-thick could be grown after 100 ALD cycles. The Ti $2p_{3/2}$ XPS peak in that case is also centered at a slightly lower binding energy, 458.4 eV, perhaps because there is still significant interference from the tungsten substrate. What is clear is that the binding energies of the Ti XPS peaks from TiO_2 show up at detectably higher values than those from the Ti^{4+} species in our titanium nitride films (458.4−459.0 versus 457.6 eV). No significant TiO_2 is formed during the $TiCl_4 + NH_3$ ALD process, so the Ti^{4+} species in that case must be associated with nitrogen, not oxygen, atoms.

3.4. Effect of the Nature of the Substrate. Finally, the effect of changing solid substrates on the titanium nitride process was briefly investigated. Four different substrates were tried, namely, glass, tungsten, nickel, and copper. XPS data from thick TiN_x films deposited on those are reported in Figure 10. The general features in the spectra are similar for all of the films, but subtle differences can be identified, in particular in the case of the glass surface. Specifically, the total amount of oxygen in the final film varies significantly across the different samples, clearly exceeding the amount of nitrogen on the glass but amounting to less than half that on copper. This trend roughly correlates with the levels of oxygen contamination present initially on the substrates before the ALD. A second variation is seen in the N/Ti ratio, which is approximately the same in the films on the three metals but slightly larger on the glass. Finally, the Ti 2p peaks in the film on glass have a larger Ti^{4+} contribution relative to the Ti^{3+} species. It is possible that in that case some TiO_2 does form during the $TiCl_4 + NH_3$ treatments. It has been reported that TiN ALD processes show considerable nucleation delays on several substrates;[33,34] that could also explain some of the results in this figure. However, the nucleation problem was not the central objective of our research, and was not explored any further.

4. Discussion

The XPS studies reported above provide some insights on the molecular details of the atomic layer deposition of titanium nitride films using titanium tetrachloride and ammonia. Below we focus on the discussion of three related aspects of this process, namely, the nature of the grown films, the details of the redox reaction involved, and the source of the impurities that often incorporate during the deposition.

Regarding the nature of the films, our XPS data clearly indicate that they consist of a mixture of TiN and Ti_3N_4. For one, they were found to always be rich in nitrogen: the N/Ti ratio was always measured to be above unity (Figure 7). In fact, even though most past publications report the deposition of TiN films, in the cases where compositional information has been provided, deviations from N/Ti = 1 can often be seen.[15,20,21,35−37] Because these deviations are not large, and because of the uncertainties associated with the measurements of surface concentrations, they have been commonly ignored. Certainly, surface atomic ratios are not very sensitive to changes in film composition and, therefore, are less than ideal as a method to determine the nature of the surface. It is the detection of Ti^{4+} species in the XPS from the films in our work (Figure 5) that

makes the case for Ti_3N_4 compelling. Ti_3N_4 is thermodynamically less stable than TiN, at least at low pressures,[38] but its formation has been suggested in other film deposition studies.[39−41]

Some past studies on TiN deposition have also reported the use of X-ray diffraction techniques for the characterization of the films,[15,20,21,36,37,42,43] but in none of those were structures other than TiN identified. However, two issues need to be considered here. First, because those analyses were carried out ex situ, it is possible that the nature of the sample may have been altered from its original structure. Exposure to air in particular is expected to lead to surface oxidation.[44] Second, the Ti_3N_4 species reported in our studies is only present as a thin upper layer on top of the TiN film. This is supported both by the appearance of the Ti^{4+} XPS signal early during the ALD film growth (Figure 5) and by its fast removal at the beginning of the depth profile analysis (Figure 6). Crystallographic techniques may not be sensitive enough to identify what is expected to be a small contribution to the total diffraction signal.

The fact that Ti_3N_4 is only seen on the topmost surface brings about another issue: that such a layer is likely to form during the $TiCl_4$ exposure half-cycle of the ALD process. This could explain why the topmost layer still contains Ti^{4+} species after the treatment with ammonia. It can be argued that $TiCl_4$ adsorption is most likely dissociative, and that it results in the formation of $TiCl_3$(ads) surface species. Certainly, those intermediates have been isolated and identified already on tungsten surfaces.[24,25] Also, some Ti^{3+} species were seen here in the initial stages of $TiCl_4$ deposition on the nickel foil (Figure 2). We propose that the initial dissociative step during the $TiCl_4$ half-cycle of the ALD process

$$TiCl_4(g) \rightarrow TiCl_3(ads) + Cl(ads) \quad (1)$$

may also be the step that leads to the reduction of the titanium. The adsorbed chlorine atoms could then perhaps recombine and desorb as Cl_2(g) or react later with ammonia to make chloroamines. The implication from this suggestion is that it is the $TiCl_4$, not the ammonia, that is the reducing agent for the formation of TiN films. This would mean that it is more important to find better, perhaps more reactive, substitutes for the source of titanium than to replace the ammonia with other nitrogen sources to improve the performance of the ALD processes. The use of alternative nitrogen sources to replace ammonia has been tried in the past with mixed results.[5,45] Attempts have also been made to substitute $TiCl_4$, typically with amine complexes, but although those seem to react at lower temperatures, they bring additional problems associated with the deposition of carbon impurities.[46−50]

Given the limited data available from our experiments, the suggestion that ammonia may not be the reducing agent in the conversion of $TiCl_4$ to TiN can only be tentative, and it is not without objections. Thermodynamically, reduction with ammonia is more favorable than with additional titanium tetrachloride. The appropriate standard Gibbs free energies for both reactions can be estimated using reported energetics[51,52] as follows:

$$3TiCl_4(g) + 4NH_3(g) \rightarrow 3TiN(s) + 12HCl(g) + {}^1/_2N_2(g)$$
$$\Delta G^\circ_{400\ ^\circ C} = -48.8\ \text{kJ/mol} \quad (2)$$

versus

$$2TiCl_4(g) + 2NH_3(g) \rightarrow 2TiN(s) + 6HCl(g) + Cl_2(g)$$
$$\Delta G^\circ_{400\ ^\circ C} = 179.4\ \text{kJ/mol} \quad (3)$$

Reaction 2 has been assumed to be the one operative in chemical vapor deposition processes,[35,42] although, to the best of our knowledge, no direct evidence has been provided for it. The same chemistry has also been assumed in ALD processes.[20,21] Nevertheless, it can be argued that the separation of the two reactants may alter the kinetics and mechanism of the overall process. It should also be kept in mind that processes with positive standard Gibbs free energies can still be driven under the operational conditions of ALD, where the products are removed from the reaction mixture and the equilibrium is shifted toward the formation of the solid.

The identification of both half steps and the overall reaction in the $TiCl_4 + NH_3$ ALD requires further investigation. Perhaps the best way to settle this issue is by directly detecting and identifying all of the byproducts from this process. Unfortunately, in the only study that attempted to do that, HCl was detected exclusively.[53] The authors of that work explicitly searched for but did not detect any molecular nitrogen production; it is not clear if they also looked for chlorine or chloroamine production. Chloroamines in particular are thermodynamically less stable than ammonia, but are isolatable, at least in aqueous form.[54] Interestingly, Juppo et al. reported the production of HCl during both half-cycles of the $TiCl_4 + NH_3$ ALD process. Perhaps some of the HCl produced during the $TiCl_4$ dose originates from these side reactions.

Finally, we turn to the deposition of impurities during the ALD growth of the titanium nitride films. The two main contaminants detected here and in previous work are chlorine and oxygen. The amounts of chlorine deposited in our films were quite small, and easily removed by light sputtering, heating, or further ammonia treatment. This chlorine is clearly adsorbed on the surface, and most likely comes from the readsorption of HCl.[15,20] Oxygen, on the other hand, is a more serious problem. Oxygen contamination has also been reported repeatedly in the past but dismissed as the result of subsequent exposure of the TiN films to air.[20,21] In our case, special care was placed not to expose the sample to air, so this explanation could be ruled out. A small amount of water was surely present in the reactor during deposition, but the formation of TiO_2 by $TiCl_4 + H_2O$ or $TiCl_4 + O_2$ ALD processes was also discarded on the basis of the significantly different binding energies recorded for the Ti^{4+} species from those processes compared to that measured for the titanium nitride films (Figure 9). In fact, because no significant amount of TiO_2 was detected in the films at all, it is still not clear what the nature of the oxygen may be. Regardless, we adventure to propose that the source of the oxygen contamination could be the original substrate. We base this proposal on the rough correlation between the levels of oxygen contamination in the original supports versus that in the grown TiN films (Figure 10). In lieu of other sources of O, as is the case in high-vacuum conditions, this seems like the most plausible explanation.

5. Conclusions

The surface chemistry of titanium nitride atomic layer deposition processes was characterized under controlled ultrahigh vacuum conditions by using X-ray photoelectron spectroscopy. The initial adsorption of $TiCl_4$ on any of the four substrates tested in this study (glass, tungsten, nickel, and copper) was found to be self-limiting, and at least partially dissociative. Exposures in the thousands of Langmuirs are required for monolayer saturation, which displays an average stoichiometry of approximately $TiCl_{3.5}$(ads). Some Ti^{3+} is produced initially during this uptake, most likely as the result

of a Ti−Cl bond dissociation, but those species appear to oxidize back to Ti^{4+} at higher coverages. Subsequent treatment with ammonia leads to the removal of most of the chlorine from the surface, although some residual Cl is manifested by a small XPS peak at 196.8 eV binding energy. Nitrogen in the form of a nitride is deposited until saturation is reached after less than $\sim 5 \times 10^4$ L. The operability of the whole ALD cycle was corroborated by XPS spectra taken after each step, including the pumping stages between the two half-reactions with the $TiCl_4$ and NH_3.

Thick titanium nitride films were deposited by repeated ALD cycles such as those described above. Deposition rates of approximately 0.04 nm/cycle were obtained under the best of conditions, but higher values were measured if proper purging between the half-cycles to avoid additional CVD was not performed. The titanium is initially deposited as Ti^{4+}, as indicated by the appearance of a peak at 457.6 eV in the XPS spectra, but Ti^{3+} (BE = 455.2 eV) becomes the prevalent species as the deposited film becomes thicker. Depth profiling analysis of the grown films indicated that the Ti^{4+} species is present only on the surface. This, together with the high (>1) N/Ti ratios observed, indicates that a Ti_3N_4 layer sits on top of the TiN films, and that the reduction of the titanium atoms may occur during the next exposure to $TiCl_4$.

Additional studies were carried out to identify the sources of contaminants in the ALD process. It was determined by mass spectrometry that $TiCl_4$ tends to partially decompose upon interaction with the walls of the reactor and to react with water adsorbed there to produce HCl. This problem can be minimized by conditioning the apparatus before use. Some water displacement and desorption from the walls is also induced by $TiCl_4$ during dosing but does not appear to affect the film growth in any significant way. It was shown that TiO_2 films could be grown via $TiCl_4 + H_2O$, and less efficiently via $TiCl_4 + O_2$, ALD cycles. However, those are characterized by Ti 2p XPS binding energies significantly higher than those in TiN films. Similar TiN layers could be grown by the $TiCl_4 + NH_3$ ALD process on a number of substrates. The levels of oxygen contamination varied with substrate, being significantly higher on glass than on any of the metals used here. It is suggested that some of the oxygen in the substrate may diffuse into the TiN films during growth.

Acknowledgment. Financial support for this research was provided by the U.S. Department of Energy.

References and Notes

(1) Rossnagel, S. M. *J. Vac. Sci. Technol., B* **1998**, *16*, 2585.
(2) Choy, K. L. *Prog. Mater. Sci.* **2003**, *48*, 57.
(3) George, S. M.; Ott, A. W.; Klaus, J. W. *J. Phys. Chem.* **1996**, *100*, 13121.
(4) Lim, B. S.; Rahtu, A.; Gordon, R. G. *Nat. Mater.* **2003**, *2*, 749.
(5) Kim, H. *J. Vac. Sci. Technol., B* **2003**, *21*, 2231.
(6) Ritala, M. Atomic Layer Deposition. In *High-k Gate Dielectrics*; Houssa, M., Ed.; Institute of Physics: Bristol, PA, 2004; pp 17−64.
(7) Ahonen, M.; Pessa, M.; Suntola, T. *Thin Solid Films* **1980**, *65*, 301.
(8) Suntola, T. *Mater. Sci. Rep.* **1989**, *4*, 261.
(9) Leskela, M.; Ritala, M. *Angew. Chem., Int. Ed.* **2003**, *42*, 5548.
(10) Gordon, R. G.; Hausmann, D.; Kim, E.; Shepard, J. *Chem. Vapor Deposition* **2003**, *9*, 73.
(11) Hiltunen, L.; Leskelä, M.; Makelä, M.; Niinistö, L.; Nykänen, E.; Soininen, P. *Thin Solid Films* **1988**, *166*, 149.
(12) Ritala, M.; Leskela, M.; Rauhala, E.; Haussalo, P. *J. Electrochem. Soc.* **1995**, *142*, 2731.
(13) Lim, J. W.; Park, H. S.; Kang, S. W. *J. Appl. Phys.* **2000**, *88*, 6327.
(14) Ahn, C. H.; Cho, S. G.; Lee, H. J.; Park, K. H.; Jeong, S. H. *Metals Mater. Int.* **2001**, *7*, 621.
(15) Uhm, J.; Jeon, H. *Jpn. J. Appl. Phys., Part 1* **2001**, *40*, 4657.
(16) Elers, K. E.; Saanila, V.; Soininen, P. J.; Li, W. M.; Kostamo, J. T.; Haukka, S.; Juhanoja, J.; Besling, W. F. A. *Chem. Vapor Deposition* **2002**, *8*, 149.
(17) Satta, A.; Schuhmacher, J.; Whelan, C. M.; Vandervorst, W.; Brongersma, S. H.; Beyer, G. P.; Maex, K.; Vantomme, A.; Viitanen, M. M.; Brongersma, H. H.; Besling, W. F. A. *J. Appl. Phys.* **2002**, *92*, 7641.
(18) Smith, S.; Li, W.-M.; Elers, K.-E.; Pfeifer, K. *Microelectron. Eng.* **2002**, *64*, 247.
(19) Gelatos, J.; Chen, L.; Chung, H.; Thakur, R.; Sinha, A. *Solid State Technol.* **2003**, *46*, 44.
(20) Kim, J.; Hong, H.; Oh, K.; Lee, C. *Appl. Surf. Sci.* **2003**, *210*, 231.
(21) Ritala, M.; Asikainen, T.; Leskelä, M.; Jokinen, J.; Lappalainen, R.; Utriainen, M.; Niinistö, L.; Ristolainen, E. *Appl. Surf. Sci.* **1997**, *120*, 199.
(22) Roth, K. M.; Yasseri, A. A.; Liu, Z. M.; Dabke, R. B.; Malinovskii, V.; Schweikart, K. H.; Yu, L. H.; Tiznado, H.; Zaera, F.; Lindsey, J. S.; Kuhr, W. G.; Bocian, D. F. *J. Am. Chem. Soc.* **2003**, *125*, 505.
(23) *Handbook of X-ray Photoelectron Spectroscopy*; Wagner, C. D., Riggs, W. M., Davis, L. E., Moulder, J. F., Muilenberg, G. E., Eds.; Perkin-Elmer Corporation: Eden Prairie, MN, 1978.
(24) Chen, W.; Roberts, J. T. *Surf. Sci.* **1996**, *359*, 93.
(25) Sandell, A.; Andersson, M. P.; Jaworowski, A. J.; Roberts, J. T.; Uvdal, P. *Surf. Sci.* **2002**, *521*, 129.
(26) Mitsui, T.; Hill, E.; Curtis, R.; Ganz, E. *J. Vac. Sci. Technol., A* **2001**, *19*, 563.
(27) Seah, M. P.; Dench, W. A. *Surf. Interface Anal.* **1979**, *1*, 2.
(28) Jeon, H.; Lee, J.-W.; Kim, Y.-D.; Kim, D.-S.; Yi, K.-S. *J. Vac. Sci. Technol., A* **2000**, *18*, 1595.
(29) Aarik, J.; Aidla, A.; Uustare, T.; Sammelselg, V. *J. Cryst. Growth* **1995**, *148*, 268.
(30) Sammelselg, V.; Rosental, A.; Tarre, A.; Niinistö, L.; Heiskanen, K.; Ilmonen, K.; Johansson, L.-S.; Uustare, T. *Appl. Surf. Sci.* **1998**, *134*, 78.
(31) Matero, R.; Rahtu, A.; Ritala, M. *Chem. Mater.* **2001**, *13*, 4506.
(32) Ferguson, J. D.; Yoder, A. R.; Weimer, A. W.; George, S. M. *Appl. Surf. Sci.* **2004**, *226*, 393.
(33) Satta, A.; Vantomme, A.; Schuhmacher, J.; Whelan, C. M.; Sutcliffe, V.; Maex, K. *Appl. Phys. Lett.* **2004**, *84*, 4571.
(34) Langereis, E.; Heil, S. B. S.; van de Sanden, M. C. M.; Kessels, W. M. M. *Phys. Status Solidi C* **2005**, *2*, 3958.
(35) Fix, R.; Gordon, R. G.; Hoffman, D. M. *Chem. Mater.* **1991**, *3*, 1138.
(36) Leutenecker, R.; Froeschle, B.; Cao-Minh, U.; Ramm, P. *Thin Solid Films* **1995**, *270*, 621.
(37) Faltermeier, C. G.; Goldberg, C.; Jones, M.; Upham, A.; Knorr, A.; Ivanova, A.; Peterson, G.; Kaoloyeros, A. E. *J. Electrochem. Soc.* **1998**, *145*, 676.
(38) Kroll, P. *J. Phys.: Condens. Matter* **2004**, *16*, S1235.
(39) Johansson, B. O.; Hentzell, H. T. G.; Harper, J. M. E.; Cuomo, J. J. *J. Mater. Res.* **1986**, *1*, 442.
(40) Tanaka, I.; Ching, W. I. Metal nitride ceramics having spinel structure and their manufacture. *Jpn. Kokai Tokkyo Koho* Pat. Appl. 2001089241, 2001.
(41) Zerkout, S.; Achour, S.; Mosser, A.; Tabet, N. *Thin Solid Films* **2003**, *441*, 135.
(42) Price, J. B.; Borland, J. O.; Selbrede, S. *Thin Solid Films* **1993**, *236*, 311.
(43) Hu, J. C.; Chang, T. C.; Chen, L. J.; Yang, Y. L.; Chang, C. Y. *Thin Solid Films* **1998**, *332*, 423.
(44) Wittmer, M.; Noser, J.; Melchior, H. *J. Appl. Phys.* **1981**, *52*, 6659.
(45) Juppo, M.; Ritala, M.; Leskela, M. *J. Electrochem. Soc.* **2000**, *147*, 3377.
(46) Musher, J. N.; Gordon, R. G. *J. Mater. Res.* **1996**, *11*, 989.
(47) Min, J. S.; Son, Y. W.; Kang, W. G.; Chun, S. S.; Kang, S. W. *Jpn. J. Appl. Phys., Part 1* **1998**, *37*, 4999.
(48) Kim, D. J.; Jung, Y. B.; Lee, M. B.; Lee, Y. H.; Lee, J. H. *Thin Solid Films* **2000**, *372*, 276.
(49) Lim, J.-W.; Park, J.-S.; Kang, S.-W. *J. Appl. Phys.* **2000**, *87*, 4632.
(50) Elam, J. W.; Schuisky, M.; Ferguson, J. D.; George, S. M. *Thin Solid Films* **2003**, *436*, 145.
(51) Cox, J. D.; Wagman, D. D.; Medvedev, V. A. *CODATA Key Values for Thermodynamics*; Hemisphere Publishing Corp: New York, 1984.
(52) Chase, M. W., Jr. *J. Phys. Chem. Ref. Data* **1998**, *Monograph 9*, 1.
(53) Juppo, M.; Rahtu, A.; Ritala, M. *Chem. Mater.* **2002**, *14*, 281.
(54) Jolly, W. L. *J. Phys. Chem.* **1956**, *60*, 507.